Soliton ratchets in sine-Gordon systems with additive inhomogeneities

V. Stehr,* P. Müller, and F. G. Mertens
Physikalisches Institut, Universität Bayreuth, 95440 Bayreuth, Germany

A. Bishop
Theoretical Division and Center for Nonlinear Studies, Los Alamos National Laboratory, Los Alamos, New Mexico 87545, USA
(Received 16 September 2008; published 3 March 2009)

We investigate the ratchet dynamics of solitons of a sine-Gordon system with additive inhomogeneities. We show by means of a collective coordinate approach that the soliton moves like a particle in an effective potential which is a result of the inhomogeneities. Different degrees of freedom of the soliton are used as collective coordinates in order to study their influence on the motion of the soliton. The collective coordinates considered are the soliton position, its width and offset, and the height of the spikes that appear on the soliton. The results of the theory are compared with numerical simulations of the full system.

DOI: 10.1103/PhysRevE.79.036601 PACS number(s): 05.45.Yv, 05.10.−a

I. INTRODUCTION

Rectification phenomena like the ratchet effect appear in various fields ranging from nanodevices to biophysics [1–4]. A simple model is a pointlike particle which is driven by deterministic or nonwhite stochastic forces with zero time average. If a temporal or spatial symmetry is broken, directional motion is possible. These particles can be generalized to spatially extended solitons. These are nonlinear waves which appear as solutions for certain equations, such as, for example, nonlinear Klein-Gordon equations. It has been shown for such systems that a ratchet effect is possible [5–9].

One possibility to break the temporal symmetry is to apply a biharmonic driving force [10,11]. Such a ratchet has been experimentally implemented in an annular Josephson junction [12] where the behavior of the fluxons, which act as solitons, can be modeled by sine-Gordon systems. Josephson junctions are very appropriate to study soliton ratchets since the motion of the fluxon can easily be measured as a voltage. Because of the Josephson equations, the voltage is proportional to the average velocity of the fluxon, which is the most important measure in the case of the ratchet. The biharmonic driving force was accomplished with microwaves. The details of this motion could be clarified by means of a collective coordinate theory [13,14].

The spatial symmetry can be broken by introducing inhomogeneities into the Klein-Gordon system, for example pointlike inhomogeneities modeled by δ functions [15,16] if the size of the inhomogeneities is much smaller than the characteristic length of the system (the Josephson penetration depth in the case of Josephson junctions). Instead of δ functions, box-shaped inhomogeneities have also successfully been used [17]. To facilitate the ratchet effect, δ functions or boxes are arranged in periodically repeated cells, where each cell contains an asymmetric array of inhomogeneities. This results in an asymmetric effective potential appearing in the collective coordinate theory. These kinds of inhomogeneities can be implemented experimentally by microshorts and microresistors in a long Josephson junction [18].

Recently, another way to break the spatial symmetry in a long Josephson junction has been used [19]. A constant current has been injected in a small region of an annular Josephson junction and extracted from the same electrode along the rest of the junction. This results in an asymmetric sawtooth potential. The velocity of the soliton can be calculated from the measured voltage. Surprisingly high voltages, which would correspond to 90% of the Swihart velocity (the maximum velocity in a Josephson junction), have been reported. In case of an *ideal* ratchet, the particle (or here the soliton) would move with unit velocity during one-half of the driving period and would not move during the second half when the driving force acts in the other direction. (Referring to the Josephson contact, this velocity is normalized with the Swihart velocity.) This results in an average velocity of 0.5, which thus represents an upper limit. Thus the high velocity value of 0.9 is doubtful and it is in question whether the measured voltage can really be interpreted as the velocity. In contrast to the experiment, we derive the velocity of the soliton from its calculated trajectory.

The aim of this paper is to study the ratchet mechanism in the case of additive inhomogeneities by means of a collective coordinate theory. In Sec. II we begin by introducing the inhomogeneous sine-Gordon system that describes the experiment. In Sec. III numerical simulations of this system are shown in order to gain a first impression of how this system behaves and to understand the *Ansätze* that we make within the collective coordinate theory. In Sec. IV the collective coordinate theory is developed for these different *Ansätze*, which lead to sets of coupled ordinary differential equations for the chosen collective coordinates. These equations describe the dynamics of the soliton that moves in an effective potential. This potential depends on the shape of the inhomogeneities. Finally, the results are summarized in Sec. V.

II. INHOMOGENEOUS SINE-GORDON SYSTEM

As noted above, a ratchet effect has recently been obtained experimentally with Josephson junctions by injecting a current into the junction [19]. This system can be described by a perturbed sine-Gordon equation [19],

*Vera.Stehr@Uni-Bayreuth.de

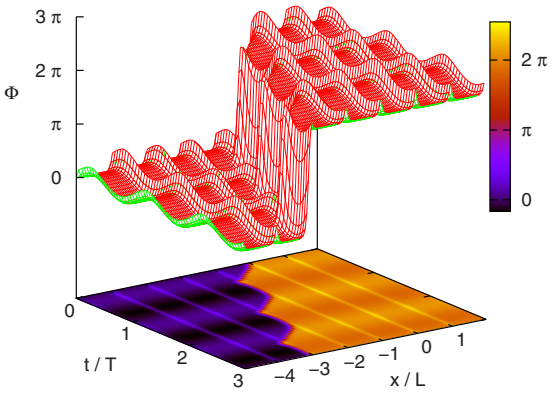

FIG. 1. (Color online) Simulation of Eq. (1). Parameters of the inhomogeneities, $L=21.8$, $w=0.14$, $g_1=15.9$; parameters of the driving force, $A=0.4$, $\omega=0.025$.

$$\phi_{tt} - \phi_{xx} + \sin\phi = -\beta\phi_t + f(t) + g(x), \tag{1}$$

where $\phi(x,t)$ is a scalar field and ϕ_x and ϕ_t are partial derivatives with respect to space and time. The terms on the right-hand side of the equation are perturbations. The first term is a dissipative term with the damping coefficient β. $f(t)$ is an external driving force whose temporal average vanishes. We have used a simple sine-shaped driving field,

$$f(t) = A\sin(\omega t), \tag{2}$$

with amplitude A and frequency ω. This corresponds to an ac bias current in the experiment. The inhomogeneity function $g(x)$ corresponds to the injected current that allows for the ratchet effect. g takes two values: a high positive one (g_1) in a small region with the width w and a small negative one $(-g_2)$ in the rest of the cell of total length L. This cell is repeated periodically:

$$g(x) = \begin{cases} g_1 & \text{for } nL < x \leqslant nL + w, \\ -g_2 & \text{for } nL + w < x \leqslant (n+1)L, \end{cases} \tag{3}$$

where n is an integer number. The spatial average of g must vanish, which results in $g_1 w = g_2(L-w)$.

III. SIMULATIONS

In order to get a first impression of the behavior of the system, simulations of the full perturbed sine-Gordon system were performed. Equation (1) was discretized with respect to the spatial coordinate x, and the resulting system of ordinary differential equations was solved by using the Heun or Runge-Kutta algorithm. The step sizes for the temporal and the spatial coordinates were $\Delta t=0.01$ and $\Delta x=0.05$, respectively. ϕ was initialized with the kink soliton solution of the unperturbed sine-Gordon equation [Eq. (1) without the terms on the right-hand side]:

$$\phi(x,t) = 4\arctan\exp\left(\frac{x - vt}{\sqrt{1-v^2}}\right) \tag{4}$$

with the kink velocity v. In order to have a better numerical stability periodic boundary conditions were used.

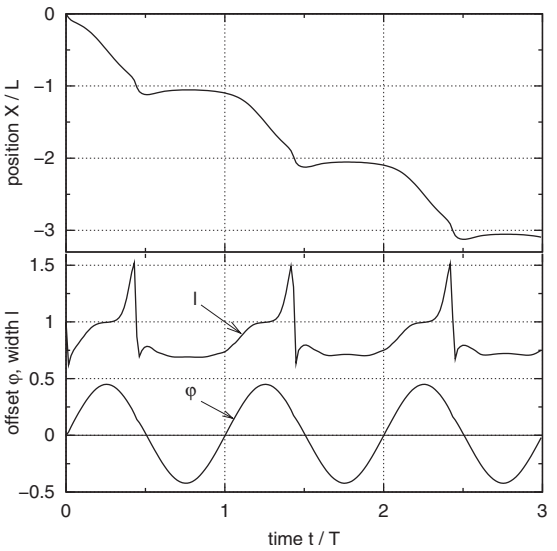

FIG. 2. Temporal development of the three fit parameters (position X, width l, and offset φ) from Eq. (5) for the kink in Fig. 1.

Figure 1 shows a simulation of Eq. (1) with a set of parameters for which a directional motion of the kink occurs. The field ϕ depending on x/L and t/T is plotted. L is the spatial period length of the inhomogeneity function $g(x)$ and $T=2\pi/\omega$ is the temporal period of the driving $f(t)$. The kink moves one spatial period per driving period in the negative direction. In addition to the movement of the kink centre in the x direction, the whole kink moves up and down with the period of the driving. Furthermore, the width of the kink (i.e., the width of the 2π step) changes during the motion. In order to determine the kink position, the kink was fitted with the function

$$\phi_{\text{fit}} = 4\arctan\exp\left(\frac{x-X}{l}\right) + \varphi \tag{5}$$

with the three fit parameters of kink center position X, kink width l, and kink offset φ. Figure 2 shows the temporal development of the fit parameters for the kink in Fig. 1.

Figure 3 shows the kink a certain time after the initializa-

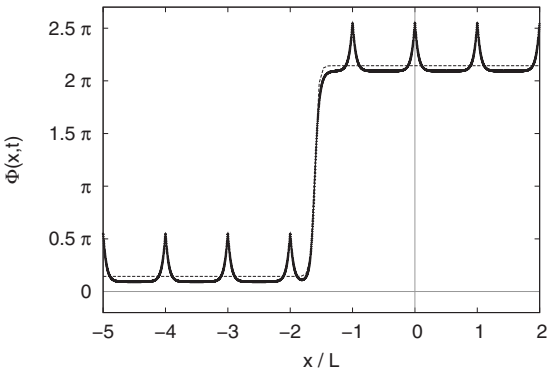

FIG. 3. The kink 300 time units after the initialization with Eq. (4). The thin line is a fit with Eq. (5). The parameters are the same as in Fig. 1.

tion with the unperturbed kink, Eq. (4). Also a fit with Eq. (5) is shown. The inhomogeneities g cause sharp peaks on the kink. They appear at the beginning of the cells where the high, narrow, positive boxes with the height g_1 are located. These spikes are stationary and do not move when the kink center moves.

For higher amplitudes, pairs of kinks and antikinks are generated which evolve from the spikes. The kinks move to the right and the antikinks to the left. When the kinks and antikinks from neighboring spikes meet, the whole kink is lifted by 2π. In such a case no ratchet effect can be observed. Furthermore, the collective coordinate theory cannot be applied. This is why the choice of parameters for the inhomogeneity and the driving is restricted to cases where no generation of kink-antikink pairs is possible. As low damping facilitates the generation, the system is studied in the case of strong damping with the damping coefficient $\beta=1$. Nevertheless, additional kinks and antikinks already appear for relatively low driving amplitudes of less than 1. This is a difference from systems with multiplicative inhomogeneities [15–17]. Hence the decisive factor for our problem is the fact that the inhomogeneities are additive. This can be understood with the aid of the pendulum model for the sine-Gordon equation [20,21]. The multiplicative inhomogeneities correspond to a locally enhanced restoring force for some of the pendulums. The additive inhomogeneities, however, correspond to a static displacement of some pendulums. That is why the spikes appear, and this of course helps the rollover of the pendulum chain. This rollover corresponds to the generation of a kink-antikink pair.

This easy kink-antikink generation that appears in the model described by Eq. (1) could be the reason for the high voltage measured in the experiment in [19] since the superconductor becomes locally normal-conducting. Yet it was observed in the simulations that for the higher frequencies which were used in the experiment it is possible that neighboring kinks and antikinks do not run into each other, since the direction of the driving and therefore the direction of the kink-antikink movement changes after a very short time so that the kinks and antikinks do not meet and lift the kink.

As shown above, three parameters are used in Eq. (5) to fit the kink in the simulation. It is suggestive to use these parameters as collective coordinates in the theory. The influence of each of these variables on the motion of the kink is analyzed in the following section. Furthermore the influence of the spikes that develop on the kink (Fig. 3) and their temporal change in height are studied.

IV. COLLECTIVE COORDINATE THEORIES

In this section a collective coordinate analysis of the soliton motion is presented. The idea of this technique for treating soliton-bearing equations is to presume that perturbations of the system mainly influence the motion of the soliton center and perhaps a few other parameters. That is why the degrees of freedom of the full system can be drastically reduced by deriving coupled equations of motion for the collective coordinates. (See [22] for a review and further references.) In the following *Ansätze* different collective coordinates are presented.

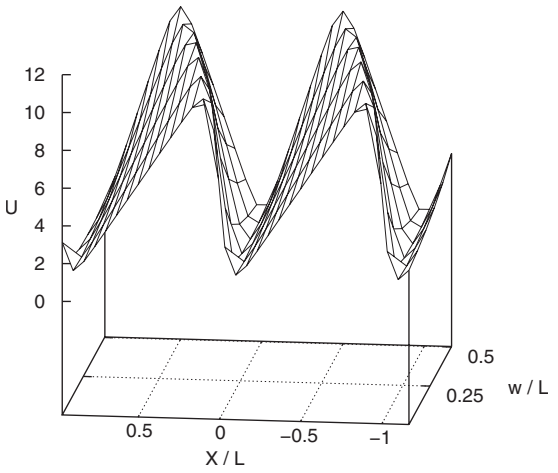

FIG. 4. Effective potential U depending on the kink position X and the width w of the positive box of $g(x)$ with value g_1. Here $g_1 w=2=\text{const}$.

A. One collective coordinate

The simplest *Ansatz* contains just the kink center position $X(t)$ as a collective coordinate (1CC *Ansatz*). The traveling wave form $\phi(x-vt)$ is generalized to $\boldsymbol{\phi}(x-X(t))$ (generalized traveling wave *Ansatz*). The soliton corresponds to a relativistic particle. With the *Ansatz*

$$\phi(x,t) = 4 \arctan \exp\left(\frac{x - X(t)}{\sqrt{1-\dot{X}(t)^2}}\right) \tag{6}$$

and the so-called adiabatic approach, first proposed by McLaughlin and Scott [18], the equation of motion can be derived with the aid of conservation laws. This leads to

$$\gamma^3 M_0 \ddot{X} + \gamma\beta M_0 \dot{X} = -qf(t) - \frac{\partial U}{\partial X}, \tag{7}$$

where $M_0=8$ and $q=2\pi$ are the soliton rest mass and topological charge, respectively. $\gamma^{-1}=(1-\dot{X}^2)^{1/2}$ is the Lorentz factor and

$$-\frac{\partial U}{\partial X} = \int_{-\infty}^{\infty} dx \frac{\partial \phi}{\partial X} g(x) \tag{8}$$

is the force due to an effective potential U. This potential cannot be calculated analytically, however. Figure 4 shows a numerical calculation. If $g(x)$ is not symmetric, i.e., if the regions with $g(x)=g_1$ and $g(x)=g_2$ have not the same width $(w \neq L/2)$, U is asymmetric as required for a ratchet effect. The smaller w [the region with $g(x)=g_1$], the stronger the asymmetry.

Figure 5 shows the movement of the kink due to the effective potential. In the plotted example, the kink moves six spatial periods into the negative direction during the first half of the driving period. When the driving, Eq. (2), changes its sign in the second half period, the kink cannot move back because it cannot overcome the steep side of U. This trajectory was confirmed by a full simulation.

Figure 6 shows the average velocity $\langle dX/dt \rangle$ of the soliton depending on the amplitude A of the driving force, Eq. (2).

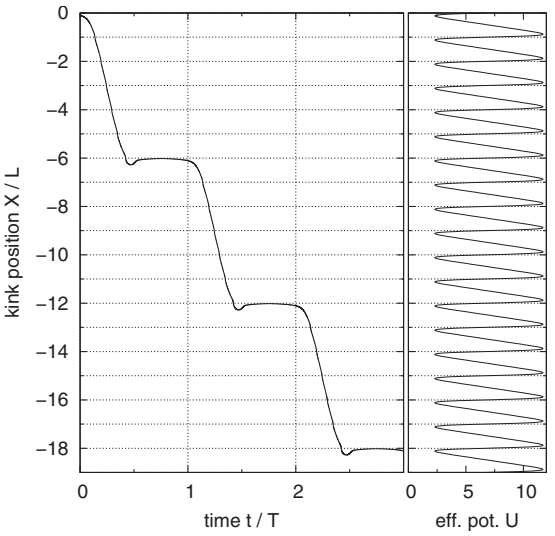

FIG. 5. Trajectory of the kink (left) and the effective potential (right) that the soliton moves in. Calculated with the 1CC *Ansatz*. Parameters: $L=21.8$, $w=0.14$, $g_1=15.9$, $\omega=0.005$, $A=0.53$.

The staircase structure is typical for ratchet systems in general [23] and has been observed for other soliton ratchets [17]. Since the soliton (or particle) travels an integer number n of spatial periods L within the effective potential during an integer number m of temporal periods $T=2\pi/\omega$ of the driving, this staircase is described by

$$\left\langle \frac{dX}{dt} \right\rangle = \frac{nL}{mT} = \frac{n}{m}\frac{L\omega}{2\pi}. \tag{9}$$

In the depicted case the soliton moves an integer number of L (n ranging from 1 to 7) during each driving period. This is why the height of the stairs always equals $L\omega/(2\pi)$. For other sets of parameters, so-called *devil's staircases* [24] have also been found, where the average velocity of the soliton changes over a cascade of rational multiples of $L\omega/(2\pi)$.

The number of steps depends strongly on the driving frequency. For small frequencies (as in Fig. 6), many steps appear. For increasing ω the step height increases [compare Eq. (9)], and the number of steps decreases accordingly.

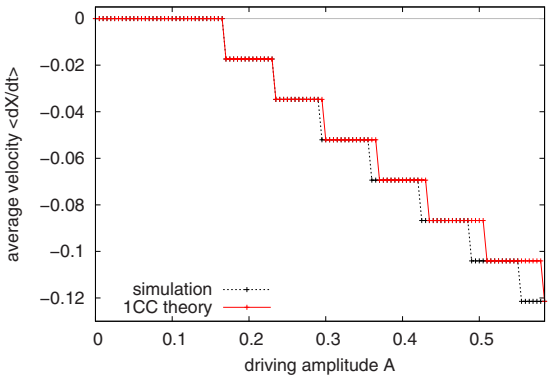

FIG. 6. (Color online) Average velocity of the kink vs driving amplitude. Comparison between 1CC theory (solid red line) and simulation (dotted black line). Parameters: $L=21.8$, $w=0.14$, $g_1=15.9$, $\omega=0.005$.

The comparison of the average velocities determined by the theory and the simulation, respectively, allows estimation of the quality of the *Ansatz* that has been used. One sees that the ratchet effect is correctly predicted by this simplest *Ansatz* with just one collective coordinate. In contrast to cases where this *Ansatz* has been applied to other sine-Gordon ratchets [15,16], even the quantitative agreement is quite good. For small amplitudes, the positions of the steps are correctly predicted. Only for higher amplitudes, the steps occur for slightly too large values of A. This also applies for other sets of parameters for the inhomogeneities and the driving.

B. Two collective coordinates

As already seen in the simulation in Sec. III, the width l of the kink is not constant. In the unperturbed case the width is subjected to only a Lorentz contraction. But in the perturbed case, the width is also influenced by the terms on the right-hand side of Eq. (1) (compare Fig. 2). Adding the kink width l as a second degree of freedom leads to the *Ansatz*

$$\phi(x,t) = 4 \arctan \exp\left(\frac{x - X(t)}{l(t)}\right). \tag{10}$$

This is the so-called *Rice Ansatz*. It was first applied to sine-Gordon and ϕ^4 solitons to study their internal modes [25]. This *Ansatz* is not an exact solution, not even for the unperturbed sine-Gordon equation. Nevertheless it has proven to be effective, e.g., for the analysis of resonances in the ϕ^4 equation [26,27]. Furthermore its excellent adequacy for sine-Gordon systems with multiplicative inhomogeneities has already been shown [15–17]. Strictly speaking l is half of the width of the kink, but, for simplicity, l is referred to as the kink width.

Applying the collective coordinate theory together with this *Ansatz* yields the two coupled equations of motion

$$M_0 l_0 \frac{\ddot{X}}{l} + \beta M_0 l_0 \frac{\dot{X}}{l} - M_0 l_0 \frac{\dot{X}\dot{l}}{l^2} = -qf(t) - \frac{\partial U}{\partial X}, \tag{11}$$

$$\alpha M_0 l_0 \frac{\ddot{l}}{l} + \beta\alpha M_0 l_0 \frac{\dot{l}}{l} + M_0 l_0 \frac{\dot{X}^2}{l^2} = K_{\mathrm{int,2CC}} - \frac{\partial U}{\partial l}, \tag{12}$$

with

$$K_{\mathrm{int,2CC}} = \frac{M_0 l_0}{2}\frac{\dot{X}^2 + 1}{l^2} + \frac{\alpha M_0 l_0}{2}\frac{\dot{l}^2}{l^2} - \frac{M_0}{2l_0}, \tag{13}$$

where $l_0=1$ is the width of the static kink and $\alpha=\pi^2/12$. These equations describe the motion of the center of mass and the expansion of a spatially deformable particle that is driven by a force $-qf(t)$ in the effective potential $U(X,l)$ that is caused by the inhomogeneities $g(x)$ and dissipates energy because of friction. The equations of motion are coupled, i.e., the collective coordinates influence each other. Hence there is an exchange of energy between the kinetic energy of the centre of mass and the internal energy of the kink. Similar to the 1CC *Ansatz*, one obtains for the effective potential $U(X,l)$

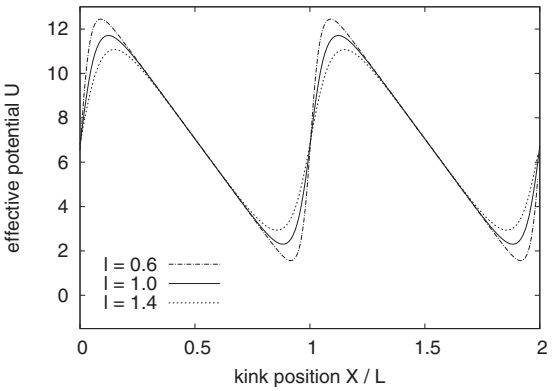

FIG. 7. Effective potential depending on the kink position for different values of the kink width. Parameters: $L=21.8$, $w=0.14$, $g_1=15.9$.

$$-\frac{\partial U}{\partial p}=\int_{-\infty}^{\infty}dx\frac{\partial \phi}{\partial p}g(x)\quad \text{with } p=X,l. \tag{14}$$

Figure 7 shows the effective potential depending on the kink position X for different values of the kink width l. The smaller l, the steeper becomes the steep side of the potential, whereas the slope of the flat side does not change. That is why the potential is higher for small values of l and vanishes if l is of the order of the spatial period length L of the inhomogeneity function $g(x)$ and U. This relation between U and l is different from the sine-Gordon system with multiplicative inhomogeneities [16]. There U decreased if l decreased. Furthermore, the shape of U changed with l: For small l there were additional small local maxima on the flat side of the potential. In the system with additive inhomogeneities studied here such effects are not observed even for strong changes of l.

Surprisingly, the kink width l as additional degree of freedom does not influence the trajectory of the kink. It was shown for sine-Gordon systems with multiplicative inhomogeneities that this second collective coordinate was crucial for quantitatively good results [15,16]. However, in the case of additive inhomogeneities, the kink width as a second degree of freedom does not improve the already quite good 1CC *Ansatz*.

A further possible *Ansatz* with two collective coordinates contains the kink offset $\varphi(t)$ instead of the kink width l:

$$\phi(x,t)=4\arctan\exp\left(\frac{x-X(t)}{\sqrt{1-\dot{X}^2(t)}}\right)+\varphi(t). \tag{15}$$

This offset is similar to the phonon dressing of the kink introduced in [28] that was caused by the driving. It was shown there that the dressing changes the shape of the kink and increases the coupling of the kink position and its width. However, this dressing was not studied as a degree of freedom.

Applying the theory now leads to the coupled equations of motion

$$\gamma^3 M_0\ddot{X}+\gamma\beta M_0\dot{X}=-q\sin\varphi-\frac{\partial U}{\partial X}, \tag{16}$$

$$\ddot{\varphi}+\beta\dot{\varphi}+\sin\varphi-f(t)=0. \tag{17}$$

It turns out that the effective potential does not depend on φ. U is the same as in the 1CC case, Sec. IV A. Equation (17) describes a damped oscillation. If φ is small so that $\sin\varphi\approx\varphi$, it can be evaluated further. After a transient time that depends on β one gets

$$\varphi=\hat{A}\sin(\omega t-\Delta) \tag{18}$$

with the amplitude

$$\hat{A}=\frac{A}{\sqrt{(1-\omega^2)^2+(\beta\omega)^2}} \tag{19}$$

and the phase shift

$$\Delta=\arctan\frac{\beta\omega}{1-\omega^2}. \tag{20}$$

In the case of small φ Eq. (16) changes to

$$\gamma^3 M_0\ddot{X}+\gamma\beta M_0\dot{X}=-q\hat{A}\sin(\omega t-\Delta)-\frac{\partial U}{\partial X}. \tag{21}$$

The only difference between this equation and Eq. (7) is that the driving $f(t)=A\sin(\omega t)$ is replaced by $\hat{A}\sin(\omega t-\Delta)$. Thus the driving acts with an effectively larger amplitude and a phase shift. The phase shift is confirmed by simulations. However, the change of the amplitude is too small to be visible in a simulation.

If A is not small, the linearization of $\sin\varphi$ is not possible. A comparison between Eq. (16) and the 1CC Eq. (7) shows that the driving force $F_{\mathrm{ac}}=-qf(t)$ is replaced by the effective driving force $F_{\mathrm{ac,eff}}=-q\sin\varphi$. If A is large, φ is also large; $\sin\varphi$, however, is limited to values between -1 and 1. Hence, for increasing A the additional energy of the driving no longer supports the traveling of the kink but only the up and down motion.

Comparison of the trajectories calculated with this *Ansatz* and those calculated with the simple 1CC *Ansatz* reveals that the kink offset as a second collective coordinate has no influence on the motion of the kink either. Consequently the quantitative description of the ratchet effect is not improved.

C. Three collective coordinates

It is possible to combine all three collective coordinates introduced so far in one *Ansatz*:

$$\phi(x,t)=4\arctan\exp\left(\frac{x-X(t)}{l(t)}\right)+\varphi(t). \tag{22}$$

Application of the collective coordinate theory now results in the three coupled equations of motion

$$M_0 l_0\frac{\ddot{X}}{l}+\beta M_0 l_0\frac{\dot{X}}{l}-M_0 l_0\frac{\dot{X}\dot{l}}{l^2}=-q\sin\varphi-\frac{\partial U}{\partial X}, \tag{23}$$

$$\alpha M_0 l_0\frac{\ddot{l}}{l}+\beta\alpha M_0 l_0\frac{\dot{l}}{l}+M_0 l_0\frac{\dot{X}^2}{l^2}=K_{\mathrm{int,3CC}}-\frac{\partial U}{\partial l}, \tag{24}$$

$$\ddot{\varphi} + \beta\dot{\varphi} + \sin\varphi - f(t) = 0, \tag{25}$$

with

$$K_{\mathrm{int,3CC}} = K_{\mathrm{int,2CC}} + \frac{M_0}{2l_0}(1 - \cos\varphi). \tag{26}$$

Equation (25) is the same as Eq. (17), which was derived without the collective coordinate l, and was already discussed above. The only difference between Eqs. (23) and (11) (derived without φ) is that now the driving $F_{\mathrm{ac}}=-qf(t)$ is replaced by the effective driving $F_{\mathrm{ac,eff}}=-q\sin\varphi$. The consequences were also already mentioned above. In Eq. (24) the only difference from Eq. (12) (without φ) is the difference between $K_{\mathrm{int,2CC}}$, Eq. (13), and $K_{\mathrm{int,3CC}}$, Eq. (26).

In order to estimate the influence of the change in K_{int}, an approximation for the homogeneous case with $g(x)=0$, strong damping ($\beta=1$), small driving frequencies ($\omega \ll 1$), and small driving amplitude is performed. As $\ddot{\varphi}$ and $\dot{\varphi}$ are of higher order than $\sin\varphi$ and $f(t)$ with respect to ω, these terms can be neglected and Eq. (25) becomes

$$\sin\varphi = f(t). \tag{27}$$

With this equation and the definition

$$P(t) := M_0 l_0 \frac{\dot{X}}{l}, \tag{28}$$

Eq. (23) (with $U=0$) can be written as

$$\dot{P} + \beta P = -qf(t). \tag{29}$$

As $\dot{P}$ is of higher order than P with respect to ω, it can be neglected. Furthermore, we assume that l oscillates in the same order with respect to ω as $f(t)$. In that case $\dot{l}$ and $\ddot{l}$ are of higher order and can also be neglected in Eqs. (24) and (26). Equation (24) then simplifies to

$$M_0 l_0 \frac{\dot{X}^2}{l^2} = \frac{M_0 l_0}{2}\frac{\dot{X}^2 + 1}{l^2} - \frac{M_0}{2l_0} + \frac{M_0}{2l_0}(1 - \cos\varphi). \tag{30}$$

This leads to

$$\frac{l_0^2}{l^2} = 1 + \frac{P^2}{M_0^2} - 2\sin^2\frac{\varphi}{2} = 1 + 0.06A^2[1 - \cos(2\omega t)] \tag{31}$$

with $M_0=8$, $q=2\pi$, and $\beta=1$. Therefore l oscillates with the frequency 2ω around the average value

$$\langle l\rangle = \frac{l_0}{\sqrt{1 + 0.06A^2}}. \tag{32}$$

The maximum value is l_0. This is confirmed by a simulation. For small A, the difference from the *Ansatz* with one collective coordinate (Sec. IV A) is rather small. With some Taylor approximations one gets

$$l = l_0\left(1 - \frac{1}{2}CA^2 + \frac{1}{2}CA^2\cos[2(\omega t)]\right). \tag{33}$$

Hence the amplitude of l is $\frac{1}{2}CA^2$ with

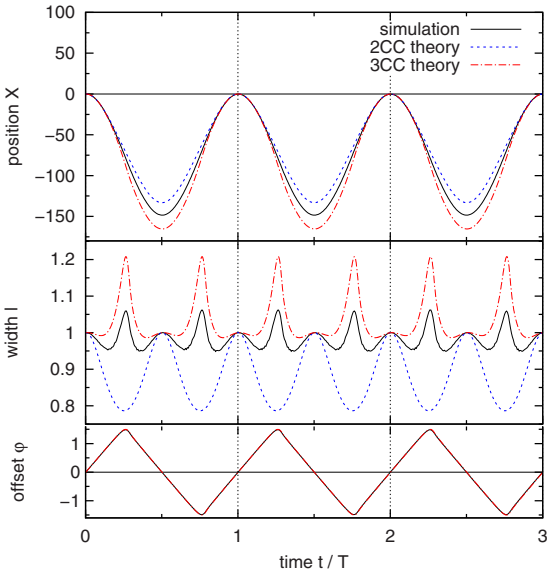

FIG. 8. (Color online) Temporal development of the three collective coordinates for $g(x)\equiv 0$ and a quite high amplitude $A=1$. The frequency is $\omega=0.01$. (Graphs that are not visible are covered by other graphs.)

$$C = \frac{q^2}{2\beta^2 M_0^2} - \frac{1}{4}. \tag{34}$$

For the trajectory one gets

$$X = \frac{qA}{\beta M_0 \omega}\left[\left(1 - \frac{3}{4}CA^2\right)\cos(\omega t) + \frac{1}{12}CA^2\cos[3(\omega t)]\right] + X_0. \tag{35}$$

X oscillates with the frequency ω. The oscillation with frequency 3ω is not observable as the term is quite small. The frequency and the amplitude of X agree very well with the simulation. For l the amplitude calculated here approximately is only about half as large as the value determined by a simulation, but the order of magnitude is predicted correctly.

For high amplitudes, the approximations made above no longer hold. Figure 8 shows a comparison of the new 3CC *Ansatz* and the 2CC *Ansatz* (with X and l) with a simulation for $g(x)\equiv 0$. The amplitude $A=1$ is chosen because for $A \geqslant 1$ the simulation of the oscillation of l shows an additional maximum at the position where a minimum appears in the case of smaller amplitudes. It is even higher than l_0. Though the exact value of this maximum differs between theory and simulation, this effect is predicted by the 3CC *Ansatz* in contrast to all other *Ansätze* made so far. For the collective coordinate φ the accordance between simulation and the two *Ansätze* is very good even quantitatively. Whereas the amplitude of the 2CC trajectory is a little too small compared to the simulation, the amplitude of the 3CC trajectory is too large by about the same amount.

Figure 9 shows the average velocity of the kink determined with the 3CC theory for the inhomogeneous case with

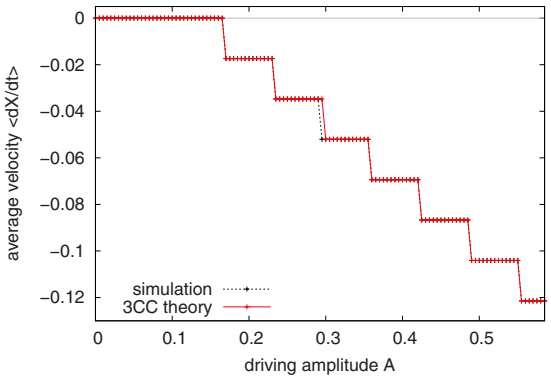

FIG. 9. (Color online) Average velocity of the kink depending on the driving amplitude, comparison between 3CC theory (solid red line) and simulation (dotted black line). Parameters are the same as in Fig. 6.

$g(x) \neq 0$. The agreement between theory and simulation has improved considerably compared to the 1CC and 2CC theories (cf. Fig. 6). The agreement between theory and simulation is now quite good even for higher amplitudes. In this 3CC *Ansatz* no new collective coordinate is introduced compared to the two 2CC *Ansätze* with X and l and X and φ, respectively. The only new feature is that here all three coordinates—X, l, and φ—are combined. Thus the crucial point seems to be the interplay between the three degrees of freedom.

D. Influence of the spikes

As already seen in the simulations (Sec. III), the inhomogeneity function $g(x)$ causes peaks on the kink (Fig. 3). The height of these peaks changes periodically. In order to test if these peaks have an influence on the kink movement, the height is introduced as a collective coordinate.

First of all the shape of the peaks has to be determined. A small perturbation $|\mu| \ll 1$ is added to the kink solution ϕ^{K}:

$$\phi(x,t) = \phi^{\mathrm{K}}(x,t) + \mu(x,t). \tag{36}$$

This is put into the perturbed sine-Gordon equation (1). As the peaks also appear on the static kink, only the static case of this equation is considered. With some approximations one gets

$$-\mu_{xx} + \mu = g(x). \tag{37}$$

In order to produce a strongly asymmetric effective potential, the width w of the region where $g(x)=g_1$ should be small (cf. Fig. 4). In such a case g can be approximated as a δ function. One has to take into account that the spatial average of g must vanish. Therefore g can be approximated as

$$g(x) = -\frac{k}{L} + \sum_n [k\delta(x - nL)], \tag{38}$$

where $k=g_1 w=g_2(L-w)$ is the area of one of the two boxes the inhomogeneity cell is built from. Solving Eq. (37) with Eq. (38) leads to

$$\mu(x) = \frac{k}{2}\sum_n e^{-|x-nL|} - \frac{k}{L}. \tag{39}$$

The *Ansatz* for the collective coordinate calculation now reads

$$\phi(x,t) = 4\arctan e^{x-X(t)} + p(t)\left(\frac{k}{2}\sum_n e^{-|x-nL|} - \frac{k}{L}\right). \tag{40}$$

For simplicity, this *Ansatz* is nonrelativistic. p is the new collective coordinate which is proportional to the height of the peaks. Applying the theory, the resulting equations of motion are

$$M_0\ddot{X} + k\left(D_1 + D_2 - 2D_3 - \frac{q}{L-4} + \frac{L}{L-4}(D_1 + D_2)\right)p - \frac{4L^2}{k(L-4)}\left(\frac{q}{L} - D_1 - D_2\right)\left(\lim_{S\to\infty}\frac{I}{S} - \frac{k(g_1-g_2)}{2L}\right) - 2\int_{-\infty}^{\infty} dx \frac{\sin\phi(X,p,x)}{\cosh(x-X)} = -M_0\beta\dot{X} - qf(t) + F_{\mathrm{inh}} \tag{41}$$

and

$$\left(\frac{k^2}{4L} - \frac{k^2}{L^2}\right)\ddot{p} + \beta\left(\frac{k^2}{4L} - \frac{k^2}{L^2}\right)\dot{p} + \frac{k^2}{4L}p - \frac{k(g_1-g_2)}{2L} + \lim_{S\to\infty}\frac{I}{S} = 0 \tag{42}$$

with

$$D_1 = \sum_n e^{X-nL}\ln(1 + e^{-2(X-nL)}), \tag{43}$$

$$D_2 = \sum_n e^{-(X-nL)}\ln(1 + e^{2(X-nL)}), \tag{44}$$

$$D_3 = \sum_n \mathrm{sech}(X - nL), \tag{45}$$

and

$$I = \int_{-S/2}^{S/2} dx \sin\phi(X,p,x)\left(\frac{k}{2}\sum_n e^{-|x-nL|} - \frac{k}{L}\right),$$

$$\lim_{S\to\infty} I \propto S, \tag{46}$$

where S is the size of the system. In Eq. (41) no derivatives of p appear. Therefore the trajectory can only be influenced by the size of the peaks but not by its dynamics. Equation (42) describes a damped oscillation of p. The variable X appears only in the integral I. This is why its influence on p and the coupling between these two equations are quite small. A numerical analysis shows indeed that p, which is initialized with the value 1, oscillates at the beginning and is damped to 0 after a short time. Consequently, the trajectory $X(t)$ is identical with the nonrelativistic 1CC trajectory, Eq. (7), with $\gamma=1$. Within the collective coordinate theory, which simplifies the soliton to a particle, the motion of the spatially

confined particle cannot influence the peaks which are spread all over the system. That is why the peak height oscillates and is damped away without being influenced by X. Since the peaks do not show any interplay with the motion of the kink center, they can be neglected in the framework of the collective coordinate theory.

V. SUMMARY AND CONCLUSIONS

The collective coordinate theory was applied previously to sine-Gordon ratchet systems with multiplicative inhomogeneities. In this work the suitability of the theory for sine-Gordon ratchets with *additive* inhomogeneities is shown. It turns out that even the simplest *Ansatz* with just one collective coordinate agrees quite well with the simulations. This is a difference from the systems with multiplicative inhomogeneities. For those systems the kink width as a second collective coordinate and the exchange between the internal energy and the translational energy were crucial for the ratchet effect. For the system with additive inhomogeneities it is shown that this second degree of freedom practically does not change the motion even though there is an influence on the effective potential.

The kink offset as a second collective coordinate instead of the kink width does not improve the theory either. The phase shift between driving and offset is correctly predicted. Furthermore, it is shown that at a certain value of the driving amplitude a further enhancement results only in a stronger up and down movement but not in a movement of the kink center. The effective potential is not influenced by the offset.

In order to improve the simplest *Ansatz* with the kink position as collective coordinate, *two* further degrees of freedom—kink width and kink offset together—are necessary. The temporal development of both the trajectory and the kink width agrees better with the simulations than with just one or two collective coordinates. The parameter values where the ratchet effect occurs are predicted more precisely. This proves that for the dynamics of the kink the interplay of all three degrees of freedom together is important.

For the homogeneous case it is shown with the *Ansatz* with three collective coordinates that the kink width oscillates with double driving frequency and does not exceed the static width as long as the driving amplitude is not too large. The amplitude of the oscillations of the soliton position is predicted quite well by the theory. The amplitude of the kink width is only half of the value in the simulation, but the order of magnitude is predicted correctly.

It is shown in the full simulations that the inhomogeneity not only influences the dynamics of the kink but also its shape. The high, narrow boxes of the inhomogeneities cause peaks on the kink. However, it is also shown that these peaks can be neglected since they have no influence on the motion of the kink.

In the case of the multiplicative inhomogeneities, the shape of the boxes could be optimized with respect to the average velocity with the aid of the collective coordinate theory [17]. This is not possible in the case of additive inhomogeneities since a local optimum does not exist. If one attempts to optimize the system in order to produce a high average velocity, the region of the amplitude where the ratchet effect occurs becomes very small and vanishes. Furthermore, the amplitude region that shows the ratchet effect moves to higher values of the amplitude. In order to get a high average velocity, one has to choose an amplitude close to the value where the generation of kinks and antikinks begins.

The generation of kinks and antikinks which evolve from the peaks caused by the inhomogeneities is made visible in the simulations. This effect occurs already for relatively small values of the amplitude. That is why the region of the parameters where the ratchet effect occurs and where the theory is valid is strongly restricted. The simulations are needed to test if the theory still works or if kink-antikink pairs are already generated.

[1] P. Hänggi and R. Bartussek, in *Nonlinear Physics of Complex Systems—Current Status and Future Trends*, edited by J. Parisi, S. C. Müller, and W. Zimmermann, Lecture Notes in Physics Vol. 476 (Springer, Berlin, 1996).

[2] F. Jülicher, A. Ajdari, and J. Prost, Rev. Mod. Phys. **69**, 1269 (1997).

[3] P. Reimann, Phys. Rep. **361**, 57 (2002).

[4] P. Reimann and P. Hänggi, Appl. Phys. A: Mater. Sci. Process. **75**, 169 (2002).

[5] I. Zapata, R. Bartussek, F. Sols, and P. Hänggi, Phys. Rev. Lett. **77**, 2292 (1996).

[6] F. Marchesoni, Phys. Rev. Lett. **77**, 2364 (1996).

[7] E. Trías, J. J. Mazo, F. Falo, and T. P. Orlando, Phys. Rev. E **61**, 2257 (2000).

[8] M. Salerno and N. R. Quintero, Phys. Rev. E **65**, 025602(R) (2002).

[9] G. Costantini, F. Marchesoni, and M. Borromeo, Phys. Rev. E **65**, 051103 (2002).

[10] S. Flach, Y. Zolotaryuk, A. E. Miroshnichenko, and M. V. Fistul, Phys. Rev. Lett. **88**, 184101 (2002).

[11] M. Salerno and Y. Zolotaryuk, Phys. Rev. E **65**, 056603 (2002).

[12] A. V. Ustinov, C. Coqui, A. Kemp, Y. Zolotaryuk, and M. Salerno, Phys. Rev. Lett. **93**, 087001 (2004).

[13] L. Morales-Molina, N. R. Quintero, F. G. Mertens, and A. Sánchez, Phys. Rev. Lett. **91**, 234102 (2003).

[14] L. Morales-Molina, N. R. Quintero, A. Sánchez, and F. G. Mertens, Chaos **16**, 013117 (2006).

[15] L. Morales-Molina, F. G. Mertens, and A. Sánchez, Eur. Phys. J. B **37**, 79 (2004).

[16] L. Morales-Molina, F. G. Mertens, and A. Sánchez, Phys. Rev. E **72**, 016612 (2005).

[17] F. G. Mertens, L. Morales-Molina, A. R. Bishop, A. Sánchez, and P. Müller, Phys. Rev. E **74**, 066602 (2006).

[18] D. W. McLaughlin and A. C. Scott, Phys. Rev. A **18**, 1652 (1978).

[19] M. Beck, E. Goldobin, M. Neuhaus, M. Siegel, R. Kleiner, and D. Koelle, Phys. Rev. Lett. **95**, 090603 (2005).
[20] A. C. Scott, Am. J. Phys. **37**, 52 (1969).
[21] M. Remoissenet, *Waves Called Solitons*, 3rd ed. (Springer, Berlin, 1999).
[22] A. Sánchez and A. R. Bishop, SIAM Rev. **40**, 579 (1998).
[23] M. Schreier, P. Reimann, P. Hänggi, and E. Pollak, Europhys. Lett. **44**, 416 (1998).
[24] A. Ajdari, D. Mikamel, L. Peliti, and J. Prost, J. Phys. I **4**, 1551 (1994).
[25] M. J. Rice, Phys. Rev. B **28**, 3587 (1983).
[26] N. R. Quintero, A. Sánchez, and F. G. Mertens, Phys. Rev. Lett. **84**, 871 (2000).
[27] N. R. Quintero, A. Sánchez, and F. G. Mertens, Phys. Rev. E **62**, 5695 (2000).
[28] C. R. Willis and M. Farzaneh, Phys. Rev. E **69**, 056612 (2004).